

Catadioptric Microlenses for Submillimeter and Terahertz Applications

Biddut K. Banik, Harald F. Merkel, Stellan Jacobsson

Abstract— Existing dielectric lens geometries are optimized for remote sensing applications in order to produce a predetermined Gaussian beam in the far field that is matched to a radioastronomic setup. In this work, an optics suitable for object investigation in a point-to-point transmission setup is presented. Here it is required to create a focus point outside the lens with as low radiation leakage as possible. For this, a catadioptric dielectric lens is proposed. This paper presents the theoretical performance of the focusing property of catadioptric lens investigated at 50 GHz and 228 GHz having $\epsilon_r = 11.7$. 3D simulation results of the catadioptric lens also show a focus point. Imaging property of catadioptric and extended hemispherical lenses are presented and compared at 50GHz. A Transient analysis of the lens is also presented.

Index Terms— Catadioptric lenses, dielectric lenses, lens antennas.

I. INTRODUCTION

DIELECTRIC lenses have found an increasing range of applications during the last years. Planar radiating or receiving elements covered by dielectric lenses are being used in millimeter and submillimeter regime [1, 2]. They also provide the capability to be integrated [3, 4] with millimeter and submillimeter planar feeding structures and electronic components such as diode detectors, oscillators, mixers etc. Due to low feed loss, ease of construction and overall size reduction, microstrip antenna-lens configurations are an attractive solution for mm-wave high gain antennas. Hemispherical, elliptical, extended hemispherical and synthesized elliptical lenses [1, 3, 4] have already been investigated and used in various applications. Matching layers [5] are also used to reduce reflection losses. Different kinds of computational methods and algorithms [4, 6-10] have been used for determining near-field [11, 12] and far-field pattern [13, 14], internal reflections [15], input impedance [16], S parameters, focusing property [17] and imaging property [18] of such dielectric lenses.

Here a transmission setup is analyzed where a current dipole radiating structure is coupled to the lens. The first goal is to minimize the dielectric lens. As a benchmark, the hemispherical, elliptical and extended hemispherical (or synthesized elliptical lens) and catadioptric geometries have been taken into account. Next, a catadioptric dielectric lens is presented here and the simulation results are compared to that of an extended hemispherical lens. It has been shown,

that dielectric lens structures with an overall size of 3-5 vacuum wavelengths still work as focusing elements.

As a next step, focusing structures have been analyzed that can be made small and offer a distinct power maximum at a certain distance from the structure. Such a focusing behavior improves the condition of subsequent inverse scattering matrices considerably.

II. LENS GEOMETRIES AND MODELING STRATEGIES

A commercial FEM electromagnetic package [19] has been used during this investigation. Firstly, simulation concentrated on 2D modeling of hemispherical, elliptical, extended hemispherical and catadioptric lenses. For all the cases, the surrounding domain around the lens is vacuum and the outer boundary conditions of the vacuum represented by Absorbing Boundary Conditions fulfilling Sommerfeld radiation conditions in the far field. In order to facilitate comparison, the lenses are always placed and centered at the respective coordinate origin.

A. Dielectric Lenses

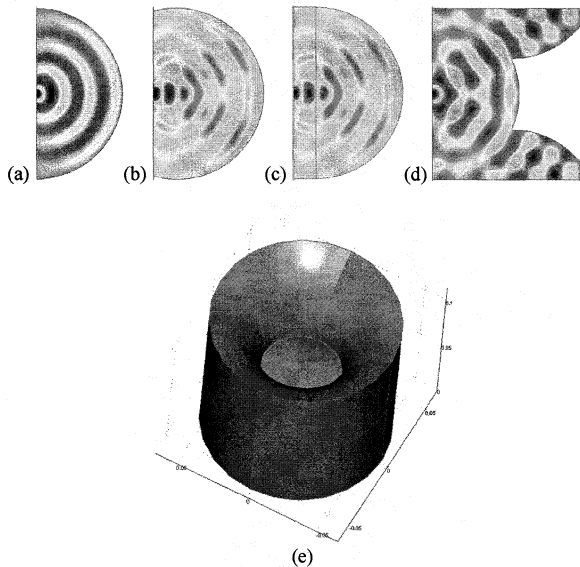


Fig. 1. Electric field distribution at 50 GHz in (a) hemispherical, (b) elliptical, (c) extended hemispherical and (d) catadioptric lens (e) 3D view of the catadioptric lens.

In Fig. 1, electric field distribution at 50GHz in hemispherical, elliptical, extended hemispherical and catadioptric lenses are shown. The dielectric constant of the lens is $\epsilon_r = 11.7$ and the lenses are of 16 mm diameter. The source is a current dipole. For the extended hemispherical lens, the extension $L = 1.6$ mm and $L/R = 0.2$ where R is the radius. The E field distributions in the elliptical and the

Manuscript received May 11, 2006.

B. K. Banik is with the Dept. of Microtechnology and Nanoscience, Microwave Electronics Laboratory, MC2, Chalmers University of Technology, Göteborg, Sweden (e-mail: biddut.banik@mc2.chalmers.se).

H. F. Merkel is with the Dept. of Microtechnology and Nanoscience, Microwave Electronics Laboratory, MC2, Chalmers University of Technology and Food Radar AB, Göteborg, Sweden (e-mail: harald.merkel@mc2.chalmers.se).

S. Jacobsson is with Food Radar AB, Göteborg, Sweden.

extended hemispherical lenses are similar. The E field distribution in the catadioptric lens indicates that the waves are guided towards the catadioptric portion. This phenomenon eventually produces a focus point.

B. Catadioptric Lens

Catadioptric lens systems have been invented by Fourier in 1826 for use in lighthouses combining a segmented Fresnel lens with lateral prisms to enhance efficiency and to reduce weight. Within the scope of the current investigation, a catadioptric lens has been realized having $\epsilon_r = 11.7$, 16 mm diameter. The extended catadioptric portion of the lens is of 8 mm radius and 11 mm length. For simplicity, two dimensional models were simulated and the lenses were assumed to be isotropic and homogenous. Fig. 2(a) shows the electric field (E_z) distribution at 50 GHz and Fig. 2(b) shows the absolute electric field (E_{norm}) distribution. A current dipole source is attached to the lens. The medium surrounding the lens is assumed to be vacuum. Fig. 2(c) shows E_{norm} along $y = 0$ axis for 48-52 GHz. The focus point

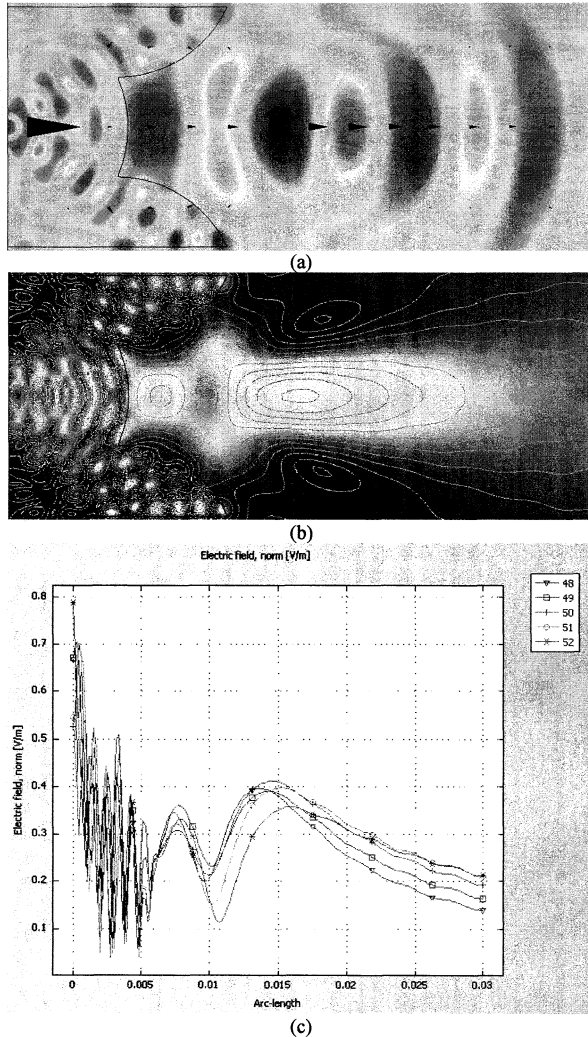


Fig.2. Field distribution at 50 GHz a) E_z b) E_{norm} c) E_{norm} along $y = 0$ axis for 48-52 GHz.

is observed at a distance $x = 0.015$ m for 50 GHz. The focusing property of the lens is frequency and lens-geometry

dependent.

Fig. 3(a) shows the normalized E_{norm} distribution at 228 GHz for the same catadioptric lens with a current dipole source. A focus point is observed at 0.0175 m. Fig. 3(b) demonstrates the normalized electric field distribution along $y = 0$ axis at 227-229 GHz.

Evidently, the quality of the calculated results depends on the density of generated mesh and the number of points where Maxwell's equations are to be solved. FEM requires very high computer resources for generating quality results at frequencies above 250 GHz, for the present case.

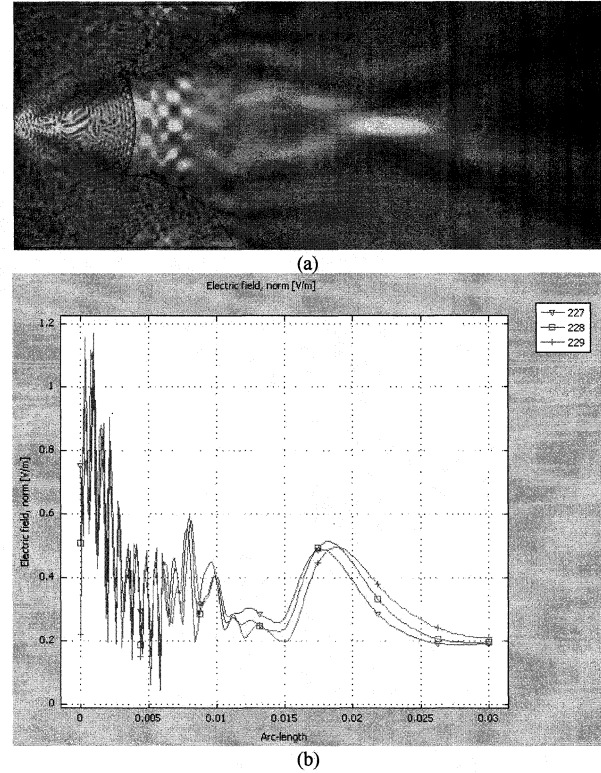


Fig.3. Field distribution at 228 GHz a) E_{norm} c) E_{norm} along $y = 0$ axis for 227-229 GHz.

C. 3D Modeling

For the 3D model of the catadioptric lens, dielectric constant $\epsilon_r = 5$, diameter $D = 16$ mm and the lens is attached to an open ended waveguide which acts as the source. The frequency is selected 28 GHz and the dimension of the waveguide is selected to be at TE_{10} mode. Higher frequency and higher dielectric constant of the lens require higher density of generated mesh, extensive amount of computer resource and eventually the simulator fails to generate any result. Fig.4 shows the isosurface plot of normalized time averaged power flow ($P_{oavnorm}$) and the color of the isosurface corresponds to the logarithm of $P_{oavnorm}$ (P_{oavdB}). Fig. 4(a) shows H plane and Fig. 4(b) shows E plane where a focus region is observed.

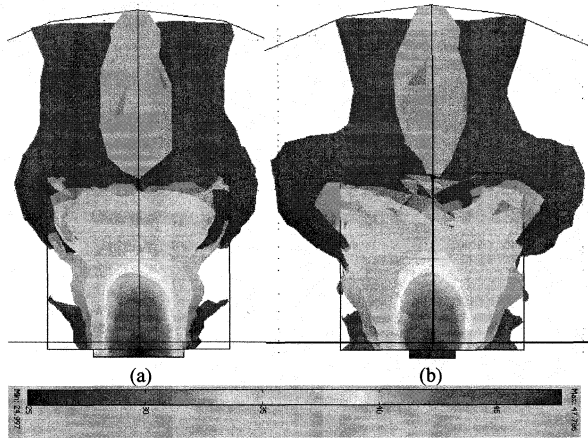


Fig. 4. Isosurface plot of normalized time averaged power flow ($P_{0avnorm}$). Waveguide source with TE_{10} excitation at 28GHz, $\epsilon_r = 5$

D. Imaging

Usually for modeling and characterizing near-field imaging setups, a planar wave is incident on the subject. For the case of catadioptric lens, a point current source is located at a distance $x = 0.016$ m, which was found to be the focus point of the lens. Fig. 5(a) shows the setup where a dielectric filled ($\epsilon_r = 11.7$) waveguide is attached to the lens and has the dimension to be excited at TE_{10} mode. The electric field distribution (E_z) is demonstrated in Fig. 5(a).

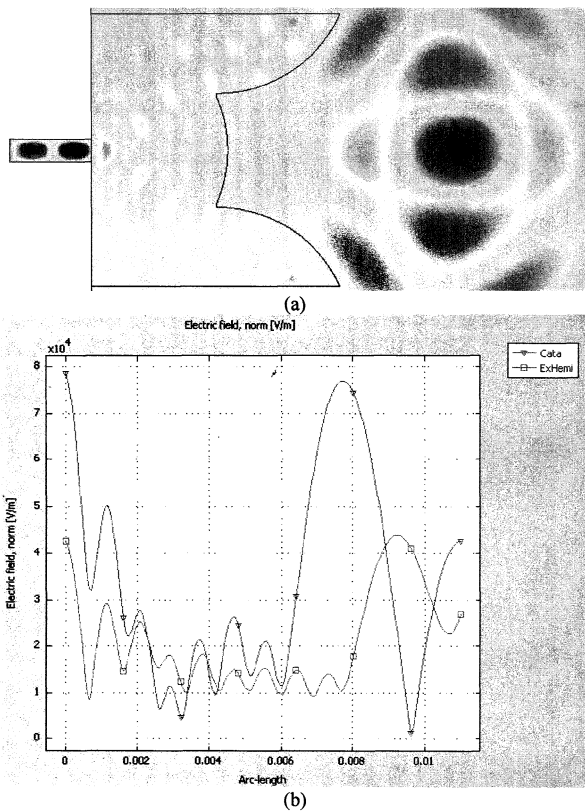


Fig. 5. (a) E_z field distribution at 50GHz with a current source located at $x = 0.016$ m. Dielectric filled waveguide is used at the receiving end. (b) E_{norm} distribution for catadioptric and extended hemispherical lenses along $y = 0$.

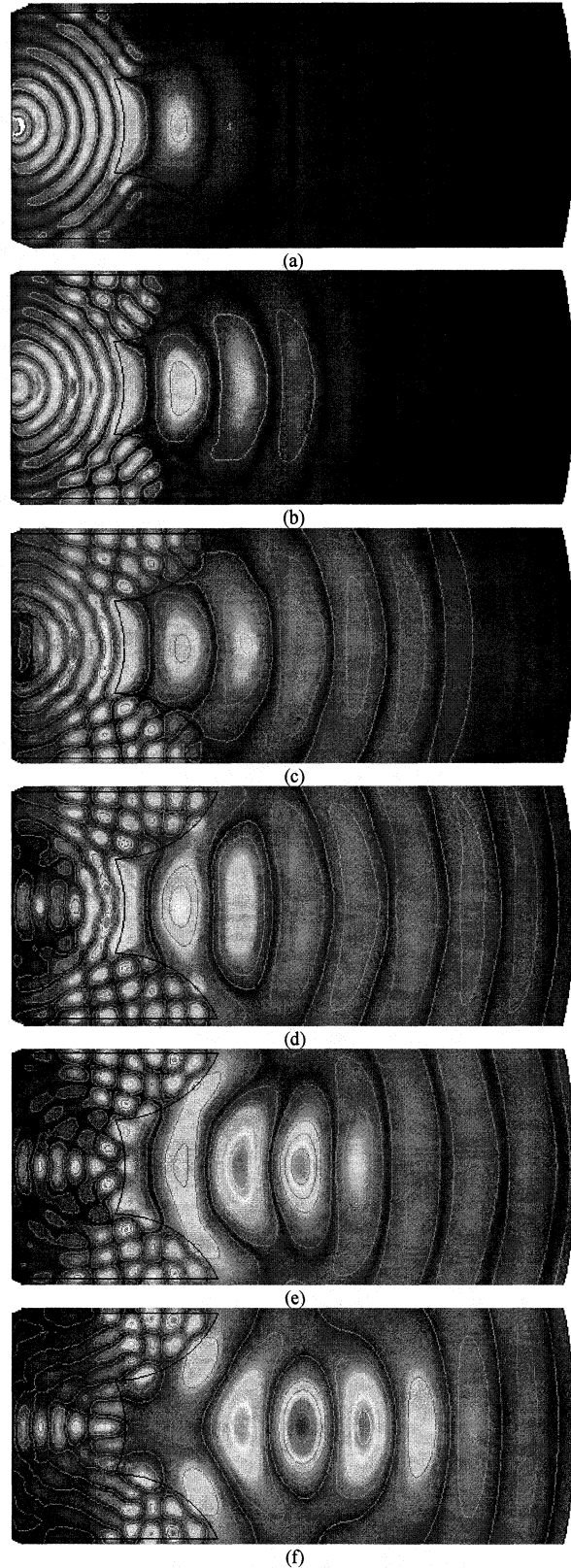


Fig. 6. Transient analysis of the catadioptric lens with a point current source located at the origin. Colors correspond to the magnitude of absolute E field distribution (E_{norm}), contour corresponds to E_z . (a) $T = 0.09$ ns (b) $T = 0.11$ ns (c) $T = 0.13$ ns (d) $T = 0.15$ ns (e) $T = 0.17$ ns (f) $T = 0.19$ ns

Afterwards, the catadioptric lens is replaced by an extended hemispherical lens having the same diameter ($D = 16$ mm) and the extension length (L) is 1.6 mm. Fig. 5(b) shows the absolute electric field (E_{norm}) distribution along $y = 0$ axis. The catadioptric lens shows approximately 3 dB better response compared to the extended hemispherical lens.

E. Transient Analysis

With a view to attain better understanding and pictorial view of the focusing property of the catadioptric lens, a transient analysis is done where a point current source is placed at the origin. It should be noted that the lens is also placed and centered at the origin. The current source generates cosine waves at 50 GHz up to the time instant $T = 0.1$ ns. Fig. 6(a-f) demonstrate the absolute electric field distribution (E_{norm}) at different time instants (0.09 ns, 0.11 ns, 0.13 ns, 0.15 ns, 0.17 ns and 0.19 ns). Fig. 6(f) shows a focus point is created at $T = 0.19$ ns.

III. CONCLUSION

The focusing property of catadioptric lens is simulated by FEM method. A 3D model also demonstrates a focus region. Nearfield imaging property is also investigated and compared to that of an extended hemispherical lens. The focusing process is presented pictorially. Our investigation results show that the catadioptric lens creates a focus point with low radiation leakage. Our future investigation encompasses introducing matching layer, reflection losses, PEC backed catadioptric lens, farfield radiation pattern, fabrication of catadioptric lenses and related measurements.

REFERENCES

- [1] L. Mall and R. B. Waterhouse, "Millimeter-wave proximity-coupled microstrip antenna on an extended hemispherical dielectric lens," *IEEE Transactions on Antennas and Propagation*, vol. 49, pp. 1769-1772, 2001.
- [2] J. Van Rudd and D. M. Mittleman, "Influence of substrate-lens design in terahertz time-domain spectroscopy," *Journal of the Optical Society of America B (Optical Physics)*, vol. 19, pp. 319-29, 2002.
- [3] D. F. Filipovic, S. S. Gearhart, and G. M. Rebeiz, "Double-slot antennas on extended hemispherical and elliptical silicon dielectric lenses," *IEEE Transactions on Microwave Theory and Techniques*, vol. 41, pp. 1738-49, 1993.
- [4] D. F. Filipovic, G. P. Gauthier, S. Raman, and G. M. Rebeiz, "Off-axis properties of silicon and quartz dielectric lens antennas," *IEEE Transactions on Antennas and Propagation*, vol. 45, pp. 760-6, 1997.
- [5] M. J. M. van der Vorst, P. J. I. de Maagt, and M. H. A. J. Herben, "Scan-optimized integrated lens antennas," Jerusalem, Israel, 1997.
- [6] J. R. Bray and L. Roy, "Physical optics simulation of electrically small substrate lens antennas," Waterloo, Ont., Canada, 1998.
- [7] A. Neto, S. Maci, and P. J. I. De Maagt, "Reflections inside an elliptical dielectric lens antenna," *IEE Proceedings-Microwaves, Antennas and Propagation*, vol. 145, pp. 243-7, 1998.
- [8] D. Pasqualini and S. Maci, "High-frequency analysis of integrated dielectric lens antennas," *IEEE Transactions on Antennas and Propagation*, vol. 52, pp. 840-847, 2004.
- [9] G. Godi, R. Sauleau, and D. Thouroude, "Performance of reduced size substrate lens antennas for Millimeter-wave communications," *IEEE Transactions on Antennas and Propagation*, vol. 53, pp. 1278-86, 2005.
- [10] B. Chantraine-Bares, R. Sauleau, L. Le Coq, and K. Mahdjoubi, "A new accurate design method for millimeter-wave homogeneous dielectric substrate lens antennas of arbitrary shape," *IEEE Transactions on Antennas and Propagation*, vol. 53, pp. 1069-82, 2005.
- [11] A. V. Boriskin, S. V. Boriskina, and A. I. Nosich, "Exact near-fields of the dielectric lenses for sub-mm wave receivers," Munich, Germany, 2003.
- [12] J. B. Pendry and S. A. Ramakrishna, "Near-field lenses in two dimensions," *Journal of Physics: Condensed Matter*, vol. 14, pp. 8463-79, 2002.
- [13] X. Wu, G. V. Eleftheriades, and T. E. Van Deventer-Perkins, "Design and characterization of single- and multiple-beam MM-wave circularly polarized substrate lens antennas for wireless communications," *IEEE Transactions on Microwave Theory and Techniques*, vol. 49, pp. 431-441, 2001.
- [14] P. Uhd Jepsen and S. R. Keiding, "Radiation patterns from lens-coupled terahertz antennas," *Optics Letters*, vol. 20, pp. 807-9, 1995.
- [15] M. J. M. Van der Vorst, P. J. I. De Maagt, A. Neto, A. L. Reynolds, R. M. Heeres, W. Luinge, and M. H. A. J. Herben, "Effect of internal reflections on the radiation properties and input impedance of integrated lens antennas - Comparison between theory and measurements," *IEEE Transactions on Microwave Theory and Techniques*, vol. 49, pp. 1118-1125, 2001.
- [16] A. Nato, L. Borselli, S. Maci, and P. J. I. de Maagt, "Input impedance of integrated elliptical lens antennas," *IEE Proceedings-Microwaves, Antennas and Propagation*, vol. 146, pp. 181-6, 1999.
- [17] W. B. Dou and E. K. N. Yung, "FDTD simulation for the focusing property of extended hemispherical lens as receiving antenna," *International Journal of Infrared and Millimeter Waves*, vol. 21, pp. 2077-86, 2000.
- [18] D. F. Filipovic, G. V. Eleftheriades, and G. M. Rebeiz, "Off-axis imaging properties of substrate lens antennas," Tucson, AZ, USA, 1995.
- [19] Comsol, www.comsol.com.